Statistical Modelling and Optimization of the Laser Percussion Microdrilling of Thin Sheet stainless Steel

Moradi, M. & Abdollahi, H.

Original citation & hyperlink:
Moradi, M & Abdollahi, H 2018, 'Statistical Modelling and Optimization of the Laser Percussion Microdrilling of Thin Sheet stainless Steel', Lasers in Engineering, vol. 40, no. 4-6, pp. 375-393.

http://www.oldcitypublishing.com/journals/lie-home/lie-issue-contents/lie-volume-40-number-4-6-2018/
ISSN 0898-1507
ESSN 1029-029X

Publisher: Old City Publishing

Statistical Modelling and Optimization of the Laser Percussion Microdrilling of Thin Sheet Stainless Steel

M. MORADI[1, 2,*] HADI ABDOLLAHI[3]

[1]*Department of Mechanical Engineering, Faculty of Engineering, Malayer University, P. O. Box 65719-95863 Malayer, Iran*
[2]*Laser Materials Processing Research Center, Malayer University, Malayer, Iran*
[3] Faculty of Mechanical Engineering, Urmia university of Technology, Urmia, Iran

*Corresponding author: Phone: +98 81 32225312 8; Fax: +98 81 32221977; E-mail: moradi@malayeru.ac.ir

Abstract

In this study, in order to investigate the influence of process parameters on the hole geometric features, the experiments were conducted based on Response Surface Methodology (RSM) as one of the most useful Design of Experiments (DOE) approaches. Frequency of laser beam (80-240Hz), duty cycle (20-40%) and laser power (100-200W) were considered as independent variables, while the entrance and exit hole diameters and their circularity as well as the hole taper were raised as process outputs. The experiments were performed on samples of thin stainless steel 321 sheet (AMS 5510) with thickness of 0.254 mm by 500W fiber laser. The results indicated that the entrance hole diameter and hole taper decrease when the laser pulse frequency increases and laser power decreases. Furthermore, laser frequency has a double reaction before duty cycle and laser powers on circularity of entrance hole. Minimum hole taper, minimum entrance diameter, and maximum circularity of entrance hole were considered as optimization criteria. Verification experiments were carried out to analyze the results obtained via software.

Key words: Statistical modeling, laser percussion drilling, micro-hole geometry features, optimization, RSM.

1 INTRODUCTION

Laser drilling process has become an industrial solution for creating micro or small hole drilling. Laser drilling is one of the main laser processing methods, with a wide range of applications [1, 2]. To name some features of this method, high speed, economic outcome and expenses can be mentioned. In recent years, laser drilling process has been the standard method to create cooling holes of aerospace components. Laser drilling relies on melting and evaporating of the material. The focused beam heats the material to the melting point. The arising melt is removed by a gas jet. Furthermore, the laser beam can heat the material to the evaporation point and the resulting material vapor escapes out of the hole. At this time, steam is formed and released; the waste comes out of the cavity and the molten walls around the cavity are formed [3]. However, holes made by laser can exhibit some defects that may restrict the application of this process in industry. Selection of input parameters of the process is to achieve desirable geometry for holes. Laser sources are widely used for engineering applications; cutting [4], drilling [5, 6], welding [7, 8] and brazing [9], recently. Performing experiments based on trial and error takes much time and does not consider the interactions of parameters, causing lots of errors. Recently, design of experiments (DOE) has been developed in various experimental works. Reduction in the number of experiments, consideration of interaction effects and development of mathematical functions to achieve the logical relationship between input and output parameters are the advantages of applying response surface methodology (RSM) [10, 11].

Mishra et al. [12] studied the effect of laser parameters on making a hole taper and heat affected zone and the depth of material removal on Nickel-base Superalloy sheet. They found that the effect of pulse frequency parameter on making a hole tapered is larger than those of the other parameters. Ghoreishi and Low [13] investigated the statistical comparison of the effect of laser

parameters on hole taper and circularity of holes which were created in laser percussion drilling on stainless steel sheets using a Nd:YAG laser source. They concluded that focal plane position in above the specimen surface, higher peak power, more pulses, more assisting gas pressure and average pulse width help to create a cylindrical hole with less hole taper. Biswas et al.[14-16] studied the laser parameters with statistical methods and found that the hole with favorable geometry with mean values of laser power, assisting gas pressure, pulse frequency and an increase in thickness is to be achieved. NG et al. [17] studied the effect of the laser percussion drilling process parameters, pulse width and laser peak power, on circularity of the hole and found that most circularity is obtained is obtained through reducing the pulse width and increasing laser power and the diameter of the hole depends on the pulse width. Kacar et al [18] experimented the effect of peak power on the hole diameter in 10mm alumina ceramic by using a Nd: YAG laser. They observed that the hole diameter increases with an increase in peak power. Jaito et al. [19] evaluated the experimental features of laser drilling with short microsecond pulses by 300 W laser fiber, continuous wave and single mode. The results showed that due to the very high brightness of the laser beam, the absorbed energy not only is enough to melt and evaporate the materials, but also is capable of separating steam in plasma at temperatures of more than 16000 Kelvin; they concluded that long pulses can enhance the quality of the hole. Low et al. [20] investigated the effects of various gases on the behavior and characteristics of spatter on the surface and recast layer for drilling with multi-pulse nimonic 263 alloy sheets using a Nd:YAG laser. It was found that the argon assist gas is significant in the structure of recast layer, which consists of several layers that alternate apertures parallel to the wall. Interlacing grain growing in the recast layer relating to main alloy was observed. laser drilling of thin steel sheet in air and underwater was studied by Nath et al. [21].

In the present study, RSM has been used to investigate the effects of laser pulse frequency, duty cycle and laser power on the geometry of the holes in laser percussion drilling. The experiments were performed using a 500W fiber laser. The thin Stainless steel 321 sheet with thickness of 0.254 mm was used as the material. Entrance and exit diameter of the created holes and their circularity as well as the hole taper of them were chosen as responses that have been analyzed by the statistical software; MINITAB 17. The obtained results indicate that the entrance hole diameter and hole taper decrease when the laser pulse frequency increases and laser power decreases. Furthermore, laser frequency has a double reaction before duty cycle and laser powers on circularity of entrance hole. Figure 1 displays a schematic of the geometrical characteristics of the hole created by laser. Optimization of the laser drilling parameters was carried out for the purpose of access proper geometrical dimensions of the created holes. In order to validate the results of optimization, drilling experiment was carried out at optimum setting and compared with the optimization results.

2 EXPERIMENTAL DESIGN AND METHODOLOGY

2.1 Response surface methodology (RSM)

Response Surface Methodology (RSM) is a set of statistical techniques and applied mathematics to investigate responses (output variables) which affected by a number of independent variables (input variables). In each experiment, changes in input variables are made in order to determine the cause of changes in the response variable. And the purpose is to find a relationship between outputs and inputs (responses and parameters) with a minimum of errors in the form of a mathematical model [23, 24]. Depending on the type of input variable parameters there are in general different ways to design an experiment. In the present study, Response Surface

Methodology is chosen as the method of design. When all the independent variables are capable of being measured and controlled during an experiment, the response surface is to be expressed as a function through Equation 1[25].

$$Y = f(x_1, x_2, x_3, \ldots, x_k) \quad (1)$$

Here, "k" is the number of independent variables. Finding a rational function to relate the independent variables to the responses seems essential. Therefore, usually a quadratic polynomial function presented in Equation 2 is applied in response surface methodology[26, 27].

$$y = \beta_0 + \sum_{i=1}^{k} \beta_i x_i + \sum_{i=1}^{k} \beta_{ii} x_i^2 + \sum_{i} \sum_{j} \beta_{ij} x_i x_j + \varepsilon \quad (2)$$

In the above Equation, β is constant, β_i is linear coefficient, β_{ii} is coefficient of quadratic, β_{ij} is interaction coefficient and ε is the error of the parameters of regression [28]. In the present study, laser pulse frequency, the duty cycle and the laser power were considered as independent input parameters. Table 1 shows three input variables of the experiment, coded values and actual values of their surfaces.

In the present study, in order to perform the experiments, central composite design (CCD) five-level RSM design with three parameters, presented in Table 2, were applied. This plan encompasses 17 experiments which include eight experiments as factorial points in the cubic vertex, six experiments as axial points and three experiments in the cubic center as center point experiments.

2.2 Desirability approach

Many response surface problems involve the analysis of several responses. Simultaneous consideration of multiple responses involves first building an appropriate response surface model for each response and then trying to find a set of operating condition that in some sense optimizes all responses or at least keeps them in desired ranges. The desirability method is recommended due to its simplicity, availability in the software and provides flexibility in weighting and giving importance for individual response. Desirability method is a simultaneous optimization technique which popularized by Derringer and Suich in 1980 [29]. Solving such multiple response optimization problems employing this technique involves using a technique for combining multiple responses into a dimensionless measure of performance called the overall desirability function [30]. The general approach is to first convert each response Yi into a unitless utility bounded by 0<di<1, where a higher di value indicates that response value Yi is more desirable, and if the response is outside an acceptable region, di=0. Then the design variables are chosen to maximize the overall desirability [31]:

$$D= (d_1.d_2\ldots.d_m)^{1/m} \quad (3)$$

Where, m is the number of responses. In the current work, the individual desirability of each response, di, was calculated using Eqs. (4-6). The shape of the desirability function depends on the weight field 'r'. Weights are used to emphasize the target value. When the weight value is equal to 1, this will make the desirability function in linear mode. Choosing r>1 places more emphasis on being close to the target value, and choosing 0<r<1 makes this less important [29]. If the target T for the response y is a maximum value, the desirability will be defined by:

$$d = \begin{cases} 0 & y < L \\ \left(\frac{y-L}{T-L}\right)^r & L \le y \le T \\ 1 & y > T \end{cases} \quad (4)$$

For goal of minimum, the desirability will be defined by

$$d = \begin{cases} 1 & y < L \\ \left(\frac{T-y}{T-L}\right)^r & L \le y \le T \\ 0 & y > T \end{cases} \quad (5)$$

If the target is located between the lower (L) and upper (U) limits, the desirability will be defined by

$$d = \begin{cases} 0 & y < L \\ \left(\frac{y-L}{T-L}\right)^r & y < L \\ \left(\frac{T-y}{T-L}\right)^r & L \le y \le T \\ 0 & y > T \end{cases} \quad (6)$$

3 EXPERIMENTAL WORK

Thin Stainless steel 321 sheet with thickness of 0.254 mm (0.1 inch) was used as experimental material workpiece. The chemical composition of the material which is the average of three X-ray fluorescence (XRF) measurements is reported in Table 3.

In the experiments a fiber laser (TLR-500-MM; IPG photonic, Ltd.) with a maximum laser power of 500 W with focus diameter of 80 μm was used as a laser source. The mode of laser is modulated or continuous wave; pulsed laser can be used in modulated mode. Focal plane position of the laser beam was fixed at 0.3 mm above the workpiece. Oxygen was used as assist gas in the experiments. Figure 2 shows the experimental set-up of the study.

Trial specimens of laser percussion drilling were performed by varying one of the process variables to determine the working range of each parameter. Small diameters in the entrance and exit holes determined were the criteria used for choosing the working ranges [32, 33]. Laser drilling experiments were performed according to matrix scheme of DOE presented in Table 2.

Figure 3 depicts the influence of the input parameters variations on the drilled geometry of some selected experiments listed in Table 2.

The entrance and exit diameters are equivalent to the entrance and exit area. Hole taper is defined by Equation 7:

$$\text{Taper}(°) = \tan^{-1}\left(\frac{d_{entrance} - d_{exit}}{2t}\right) \times \frac{180}{\pi} \quad (7)$$

Where the $(d_{entrance})$ is entrance hole diameter, (d_{exit}) is exit hole diameter, and t is the thickness of the material. The geometry features of the entrance and exit hole diameters were measured using Axioskop 40 optical microscope at a magnification of 940×. The entrance and exit diameter and circularity of each hole were exactly measured by the visilog software.

4 RESULTS AND DISCUSSION

The results of measuring the entrance and exit hole diameters and their circularities, and hole taper were considered as the responses of the experiment. Analysis of variance (ANOVA) was employed in order to investigate significant effective parameters on laser drilling process and to interpret the effect of the results. The results show that by controlling the input process parameters the proper responses could be achieved. In this analysis, full quadratic polynomial function was used.

4.1 Entrance hole diameter

According to analysis of variance on entrance hole diameter, Table 4, the only effective parameters, are laser frequency (F), and laser power (P). None of the interaction and quadratic terms were significant. The regression Equation obtained is evaluated as significant and Lack-of-Fit as insignificant. In the best analysis, regression is to be significant and Lack-of-Fit insignificant.

Therefore according to the analysis, the final regression in terms of coded parameters values yields in Equation (8).

Di(μm) = 463.69 + 26.60 P - 31.59 F **(8)**

Figure 4 illustrates response surfaces of entrance hole diameter in terms of significant input parameters. As it is observed in Figure 3 the largest diameter of the entrance hole is achieved in the highest laser power and lowest frequency [34]. The residual plot for entrance hole diameter is displayed in Figure 5. As it is shown in the normal probability diagram, the response entrance hole diameter, in comparison to others around the diagonal line, is scattered and shows a normal distribution. Therefore, the final extracted regression model is a suitable model for prediction and investigation of the effects of parameters in proportion to other responses. Thus, the result of mathematical Equation is a desirable model to predict and investigate the effect of F-test and T-test using the experiment parameter. An F-test is any statistical test in which the test statistic has an F-distribution under the null hypothesis. A t-test is any statistical hypothesis test in which the test statistic follows a student's t-distribution if the null hypothesis is supported.

4.2 Circularity of entrance hole

Table 5 shows analysis of variance for the entrance hole circularity. As shown in Table 5, among the interaction effect, between laser power and frequency (P×F), and duty cycle and frequency (F×D) were identified as the significant terms. All of the main effects and quadratic terms were insignificant. As Table 5 indicates, Lack-of-Fit was determined as insignificant and it shows that a suitable analysis has been performed. According to the performed analysis in ANOVA Table 5,

Equation 9 represents the regression Equation for the entrance hole circularity considering significant parameters based on coded values.

Circularity-in = 0.79593 - 0.00294 P + 0.00581 F - 0.00392 D + 0.02462 P×F + 0.01212 F×DT (9)

In Figure 6 and 7, the interaction between the effects of parameters in different levels and their effect on circularity of the entrance hole is displayed. In the diagram of Figure 6, the duty cycle indicates a double reaction before laser frequency. In the lowest frequency, the circularity decreases as the duty cycle increases, while this behavior in the highest point of frequency is inverse. This different behavior is seen in the diagram of Figure 6 for laser frequency and laser power.

4.3 Exit hole diameter

According to the statistical analysis the only effective parameter on the exit hole diameter is the laser power and none of the other interaction and quadratic terms are significant. Equation 10 denotes the regression Equation for the exit hole diameter considering in coded values:

$$Do\ (\mu m) = 402.53 + 20.08\ P \quad (10)$$

4.4 Circularity of exit hole

Table 6 shows variance analysis of the exit hole circularity. As it could be seen in Table 6, the effective terms are main parameter of duty cycle and the interaction effect between laser power and duty cycle (P×D), and duty cycle and frequency (F×D). Final regression Equation of the exit hole circularity, based on the significant parameters in coded values, is shown in Equation (11).

$$\text{Circularity-out} = 0.64248 + 0.00675\ P + 0.00813\ F + 0.02525\ D - 0.0365\ P\times D - 0.0487\ F\times D \quad (11)$$

In Figure 8 and 9, the interaction between the effects of factors in different levels and their effect on circularity of the exit hole is exhibited. In the diagram of Figure 8, the laser frequency indicates a double reaction before duty cycle. In the lowest duty cycle, the circularity increases as the laser frequency increases, while this behavior in the highest point of frequency is inverse. This different behavior is realized in the diagram of Figure 8 for laser power and duty cycle.

4.5 Hole taper

Table 7 shows variance analysis of the hole taper. The significant terms are the laser power and the laser frequency while the significant quadratic effects are the quadratic term of laser power (P^2) and the quadratic term of laser frequency (F^2). Final regression Equation of the hole taper, based on the significant terms in coded values, is shown in Equation 12.

$$\text{Taper} = 0.05939 + 0.01820\ P - 0.04947\ F + 0.01665\ P^2 + 0.03764\ F^2 \quad (12)$$

The diagram in Figure 10 shows the changes of hole taper based on the two parameters of laser power and laser frequency. This diagram indicates that the smallest hole taper happens in the highest frequency and lowest laser power.

5 OPTIMIZATION

By statistical analysis of data obtained from experimental tests, regression Equations explain logical relations between input variables and responses. The response optimizer option within the DOE module of Minitab statistical software package, release 17, has been used here to optimize input parametric combinations resulting in the most desirable compromise between different responses using desirability function as mentioned in section 2.2. Table 8 summarizes criterions in order to optimize process parameters. Minimum hole taper, maximum circularity of entrance hole, and minimum entrance hole diameter are the criteria of the optimization.

In the optimization procedure presented in Table 8, the importance values of the responses are mentioned. Figure 11 shows the visual representation of the optimization result. The optimization plot displays the effect of each parameter (columns) on the response or composite desirability (rows).

Verification experiment was performed at the obtained optimal input parametric setting to compare the actual responses with those as optimal responses obtained from optimization. Table 9 presents the optimal setting and the optimization results along with experimentally obtained responses and their percentage relative verification errors. It is clear that the error percentage of the study is good for engineering applications.

6 CONCLUSIONS

In the present study, the process of laser percussion drilling was performed by fiber laser on stainless steel sheet with thickness of 0.254 mm (0.1 inch). The obtained data from the experiments were analyzed through DOE. Regarding the performed experiments and statistical analyses, the following conclusions can be drawn:

1-Developed curvature of the response surface provides an appropriate RSM. In addition, it shows that the parameters of the process have been selected properly and optimized configuration of the concerned parameters has existed.

2- The entrance hole diameter and hole taper decrease when the laser pulse frequency increases and laser power decreases.

3- Laser frequency has a double reaction before duty cycle and laser powers on circularity of entrance hole.

4- By performing an optimization process, using desire ability approach, the following settings can be described as the optimum settings of the laser percussion drilling process: laser pulse frequency (F) = 240 Hz, duty cycle (D) = 26.26 % and laser power (P) = 174.74 W.

References:

1. Yilbas B.S., Sami M., Kar A.K. and Sahin A.Z., First- and second-law efficiencies for laser drilling of stainless steel. Energy 21(3) (1996) 197-203.
2. Crafer R. and Oakley P.J. Laser Processing in Manufacturing. London: Chapman & Hall. 1993.
3. Yilbas, B.S. Laser drilling : practical applications. Heidelberg ; New York : Springer. 2013.
4. Moradi M., Mehrabi O., Azdast T., Benyounis K. Y. Effect of the focal point position on CO2 laser beam cutting of injection molded polycarbonate sheets, Second International Seminar on Photonics, Optics, and Its Applications, Vol. 10150, No. 1, pp. 101500F-1-10, 2016.

5. Moradi M., Mohazabpak A. Statistical modelling and optimization of laser percussion micro-drilling on Inconel 718 sheet using response surface methodology (RSM). Journal of lasers in Engineering. (2017), Article in press.
6. Moradi M., Mohazabpak A., Khorram A. An Experimental Investigation of the Effects of Fiber Laser Percussion Drilling: Influence of Process Parameters. International Journal of Advanced Design and Manufacturing Technology 9(4) (2016), 7-12.
7. Moradi M., Ghoreishi G., Torkamany M.J., Sabbaghzadeh J., Hamedi, M.J. An Investigation on the effect of pulsed Nd:YAG laser welding parameters of stainless steel 1.4418. Advanced Materials Research 383 (2012), 6247-6251.
8. Moradi M., Ghoreishi M., Torkamany M.J. Modeling and optimization of nd:yag laser-tig hybrid welding of stainless steel. Journal of lasers in Engineering 27(3/4) (2014), 211–230.
9. khorram A., Jafari A., Moradi M. Laser brazing of 321 and 410 stainless steels using BNi-2 nickel-based filler metal. Modares Mechanical Engineering 17(1) (2017), 129-135.
10. Eltawahni H.A., Olabi A.G., Benyounis K.Y. Effect of process parameters and optimization of CO 2 laser cutting of ultra high-performance polyethylene. Materials & Design 31(8) (2010), 4029-4038.
11. Tedesco S., Benyounis K.Y., Olabi. A.G. Mechanical pretreatment effects on macroalgae-derived biogas production in co-digestion with sludge in Ireland. Energy 61(1) (2013), 27-33.
12. Mishra S. and Yadava V. Modeling and optimization of laser beam percussion drilling of thin aluminum sheet. Optics & Laser Technology **48**(0) (2013), 461-474.

13. Ghoreishi M., Low D.K.Y. and Li L. Comparative statistical analysis of hole taper and circularity in laser percussion drilling. International Journal of Machine Tools and Manufacture 42(9) (2002), 985-995.
14. Biswas R., Kuar A.S. and Mitra S. Multi-objective optimization of hole characteristics during pulsed Nd:YAG laser microdrilling of gamma-titanium aluminide alloy sheet. Optics and Lasers in Engineering 60 (2014), 1-11.
15. Biswas R., Kuar A.S, Sarkar S., Mitra S. A parametric study of pulsed Nd:YAG laser micro-drilling of gamma-titanium aluminide. Optics & Laser Technology 42(1) (2010), 23-31.
16. Biswas R., Kuar A.S., Biswas S.K., Mitra S. Characterization of hole circularity in pulsed Nd: YAG laser micro-drilling of TiN–Al2O3 composites. The International Journal of Advanced Manufacturing Technology 51(9-12) (2010), 983-994.
17. Ng G.K.L., Li L. The effect of laser peak power and pulse width on the hole geometry repeatability in laser percussion drilling. Optics & Laser Technology **33**(6) (2001), 393-402.
18. Kacar E., Mutlu S.M., Akman E., Sinmazcelik T. Characterization of the drilling alumina ceramic using Nd:YAG pulsed laser. Journal of Materials Processing Technology **209**(4) (2009), 2008-2014.
19. Tu J., Paleocrassas A.G., Reeves N., Rajule N. Experimental characterization of a micro-hole drilling process with short micro-second pulses by a CW single-mode fiber laser. Optics and Lasers in Engineering **55** (2014), 275-283.

20. Low D.K.Y., Li L., Corfe A.G. Effects of assist gas on the physical characteristics of spatter during laser percussion drilling of NIMONIC 263 alloy. Applied Surface Science **154–155(1-4)** (2000), 689-695.
21. Nath A. K., Hansdah D., Roy S. and Roy C.A. A study on laser drilling of thin steel sheet in air and underwater. Journal of applied physics 107(12) (2010), 123103 - 123103-9.
22. Golchin E., Moradi M., Shamsaei S. Laser drilling simulation of glass by using finite element method and selecting the suitable Gaussian distribution. Modares Mechanical Engineering 15(13) (2015), 416-420.
23. Montingelli M.E., Benyounis K.Y., Quilty B., Stokes J., Olabi A.G. Influence of mechanical pretreatment and organic concentration of Irish brown seaweed for methane production. Energy 118(1) (2017), 1079-1089.
24. Eltawahnia H.A., Haginob M., Benyounis K.Y., Inoueb T., Olabi A.G. Effect of CO_2 laser cutting process parameters on edge quality and operating cost of AISI316L. Optics & Laser Technology 44(4) (2012), 1068–1082.
25. Eltawahni H.A., Olabi A.G., Benyounis K.Y. Investigating the CO_2 laser cutting parameters of MDF wood composite material. Optics & Laser Technology 43(3) (2011), 648–659.
26. Montgomery D.C. Design and analysis of experiments, 7^{th} edn. Wiley, New York. (2009).
27. Moradi M., Ghoreishi M. Influences of Laser Welding Parameters on the Geometric Profile of Ni-Base Superalloy Rene 80 Weld-Bead. International Journal of advanced manufacturing Technology 55(1-4) (2011), 205-215.

28. Moradi M., Salimi N., Ghoreishi M., Abdollahi H., Shamsborhan M., Frostevarg J., Ilar T., Kaplan A.F.H. Parameter dependencies in laser hybrid arc welding by design of experiments and by a mass balance. Journal of Laser Applications 26(2) (2014), 022004-1-9.
29. Derringer G., Suich R. Simultaneous optimization of several response variables. J. Qual. Technol. 12(4) (1980), 214-219.
30. Khuri A.I. and Cornell J.A. Response Surfaces: Designs and Analyses: Second Edition: Taylor & Francis. (1996).
31. Moradi M., Golchin E. Investigation on the effects of process parameters on laser percussion drilling using finite element methodology; statistical modelling and optimization. Latin American Journal of Solids and Structures 14(3) (2017), 464-484.
32. Mohazab Pak A., Moradi M. Hole geometry features analysis in fiber laser percussion drilling process. International Journal of Advances in Mechanical & Automobile Engineering 2(1) (2015), 18-21.
33. Kuar A.S., Doloi B. and Bhattacharyya B. Modelling and analysis of pulsed Nd:YAG laser machining characteristics during micro-drilling of zirconia (ZrO2). International Journal of Machine Tools and Manufacture 46(12–13) (2006), 1301-1310.
34. Ahn D.G. and Jung G.W. Influence of process parameters on drilling characteristics of Al 1050 sheet with thickness of 0.2 mm using pulsed Nd:YAG laser. Transactions of Nonferrous Metals Society of China **19(1) (**2009**),** s157-s163.

List of FIGURES:

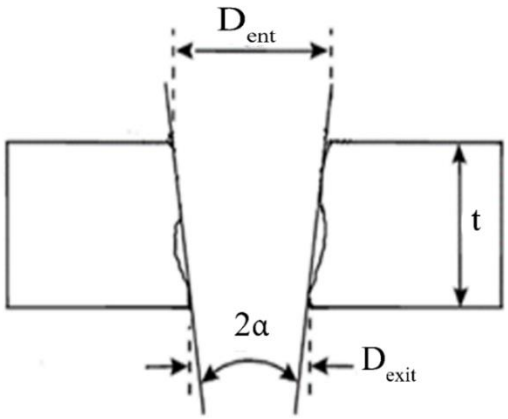

FIGURE 1.

Geometrical features of cross-section of the hole [22]

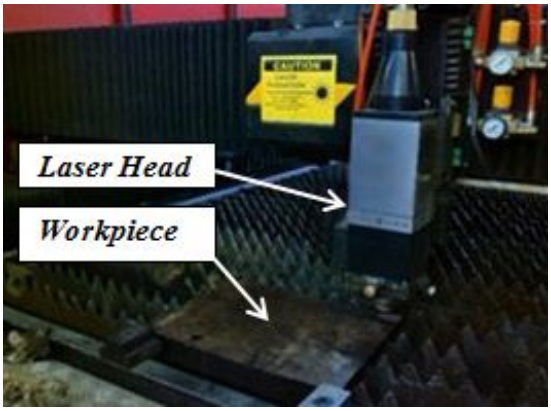

FIGURE 2.

Experimental set-up of laser drilling

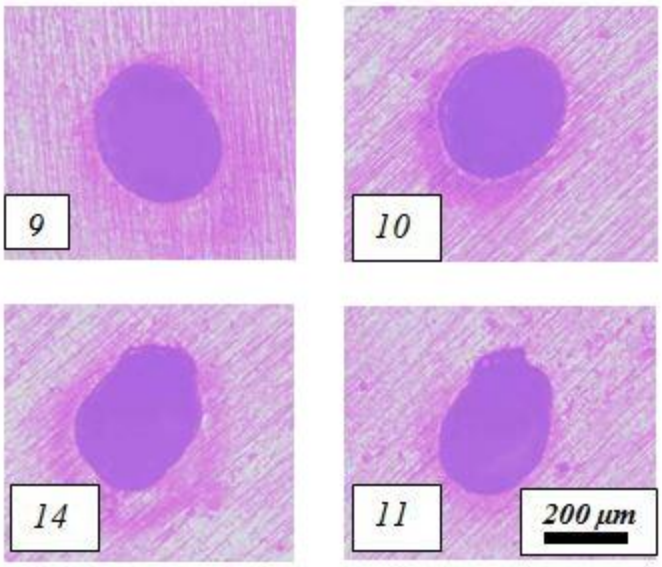

FIGURE 3.

Effect of the input parameters variations on drilled geometry

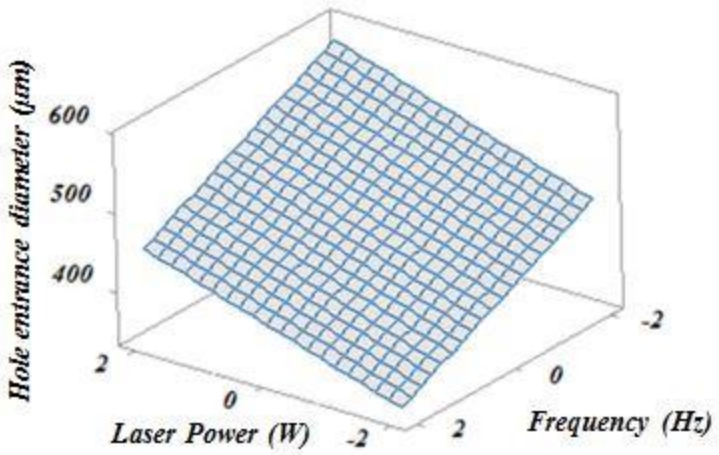

FIGURE 4.

Response surfaces of hole entrance diameter in terms of laser frequency and laser power

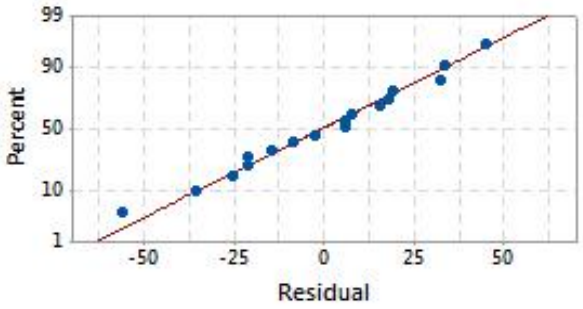

FIGURE 5.
The residual plot for hole entrance diameter

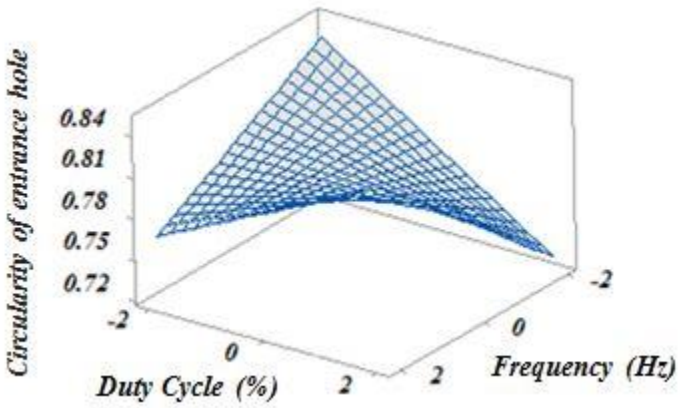

FIGURE 6.

Response surfaces of entrance hole circularity in terms of laser frequency and duty cycle

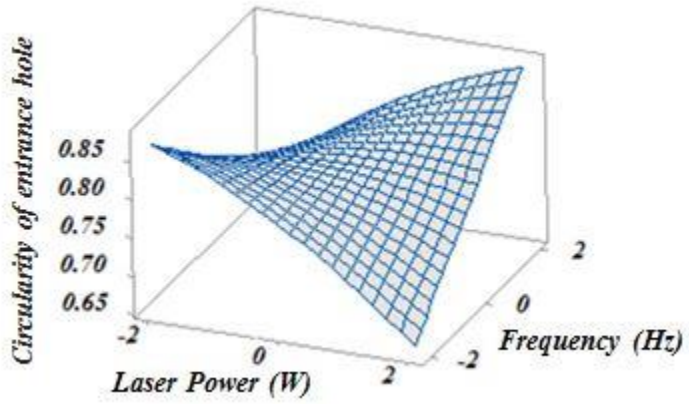

FIGURE 7.

Response surfaces of entrance hole circularity in terms of laser frequency and laser power

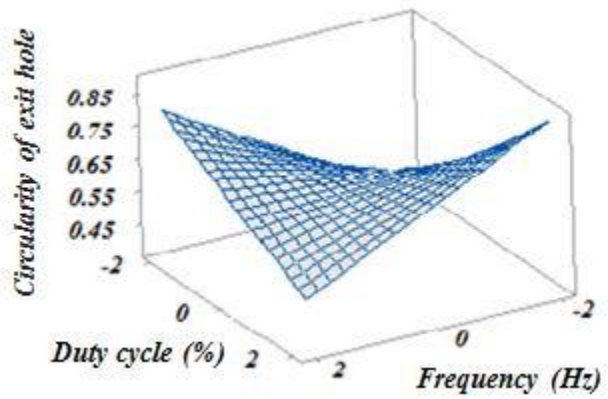

FIGURE 8.

Response surfaces of exit hole circularity in terms of laser frequency and duty cycle

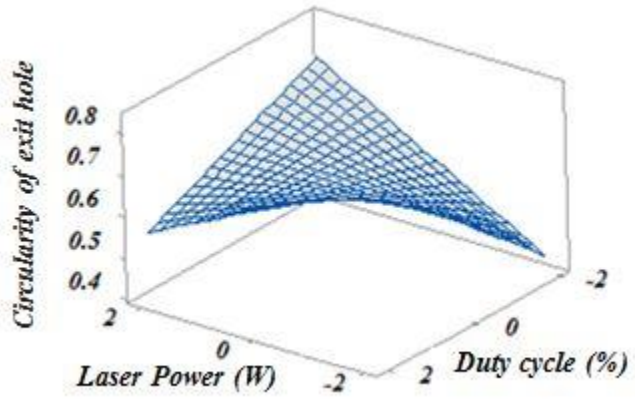

FIGURE 9.

Response surfaces of exit hole circularity in terms of laser power and duty cycle

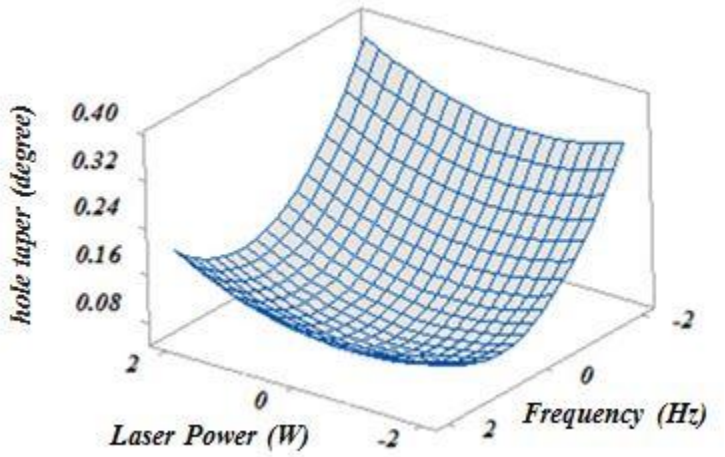

FIGURE 10.

Response surfaces of hole taper in terms of laser power and laser frequency

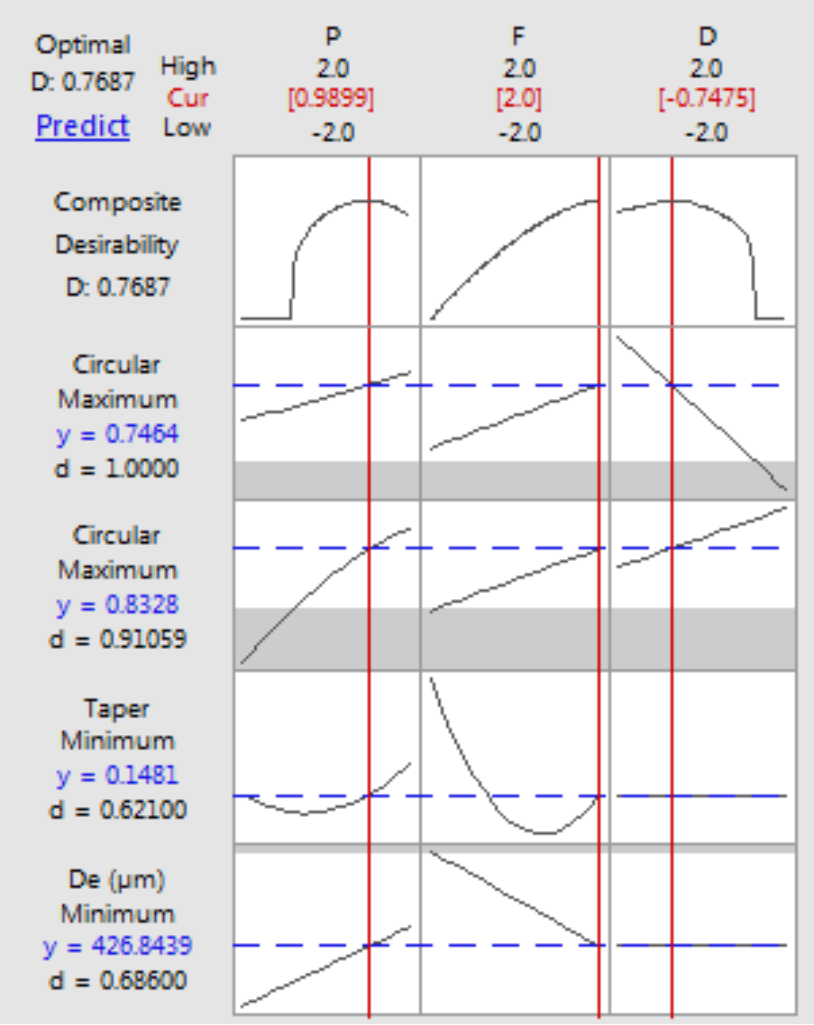

FIGURE 11.

Calculation of optimal parameters

List of TABLES:

TABLE 1

Independent process parameters with design levels

Variable	Notation	Unit	-2	-1	0	1	2
Frequency	F	[Hz]	80	120	160	200	240
Duty Cycle	D	[%]	20	25	30	35	40
Laser power	P	[W]	100	125	150	175	200

TABLE 2

Design matrix

Experiment No.	Input Parameters			Output Parameters				
	Laser power [W]	Frequency [Hz]	Duty cycle [%]	Entrance hole diameter (μm)	Exit hole diameter (μm)	Hole taper (degree)	Circularity-in	Circularity-out
1	-1	1	-1	370.21	350.02	0.04	0.774	0.656
2	2	0	0	550.57	453.74	0.19	0.771	0.66
3	0	0	0	469.70	427.38	0.08	0.797	0.6402
4	0	0	0	438.53	407.42	0.06	0.821	0.638
5	0	0	-2	471.42	433.87	0.07	0.813	0.562
6	0	0	2	461.34	380.44	0.16	0.7711	0.675
7	1	-1	1	513.71	428.30	0.17	0.749	0.666
8	1	-1	-1	537.39	455.75	0.16	0.762	0.599
9	-1	-1	1	454.13	400.84	0.10	0.804	0.746
10	-1	-1	-1	447.41	364.06	0.16	0.829	0.529
11	1	1	-1	402.70	375.12	0.05	0.797	0.696
12	0	0	0	469.77	447.48	0.04	0.793	0.723
13	0	2	0	445.60	387.00	0.12	0.789	0.676
14	1	1	1	437.46	403.52	0.07	0.841	0.572
15	-2	0	0	428.53	386.62	0.08	0.771	0.57
16	0	-2	0	546.15	380.68	0.33	0.771	0.64
17	-1	1	1	438.00	360.71	0.15	0.789	0.674

TABLE 3
Chemical Composition of Stainless Steel 321 AMS 5510 (Wt.%)

Fe	Ni	Cr	N	Mo	Ti	Mn	Si	C	P	S
Bal	12	18	0.1	0.75	0.65	1.95	0.85	0.08	0.04	0.03

TABLE 4

Revised analysis of variance of hole entrance diameter

Source	DF	Adj SS	Adj MS	T-Value	F-Value	P-Value
Model	٢	27283.4	13641.7	-	16.61	0.000
Linear	٢	27283.4	13641.7	-	16.61	0.000
F	1	15962.9	15962.9	-4.41	19.44	0.001
P	1	11320.5	11320.5	3.71	13.79	0.002
Error	١٤	11495.8	821.1	-	-	-
Lack-of-Fit	١٢	10846.7	903.9	-	2.79	0.294
Pure Error	٢	649.1	324.6	-	-	-
Total	١٦	38779.3	-	-	-	-
R-sq(adj) =66.12%	R-sq = 70.36**%**					

TABLE 5

Revised analysis of variance of entrance hole circularity

Source	**DF**	**Adj SS**	**Adj MS**	**T-Value**	**F-Value**	**P-Value**
Model	۶	0.007720	0.001287	-	5.48	0.009
Linear	۳	0.000925	0.000308	-	1.31	0.324
P	1	0.000138	0.000138	-0.77	0.59	0.461
F	1	0.000541	0.000541	1.52	2.30	0.160
D	1	0.000246	0.000246	-1.02	1.05	0.330
2-Way Interaction	2	0.006027	0.003014	-	12.83	0.002
P×F	1	0.004851	0.004851	4.54	20.65	0.001
F×D	1	0.001176	0.001176	2.24	5.01	0.049
Error	10	0.002349	0.000235	-	-	-
Lack-of-Fit	8	0.001891	0.000236	-	1.03	0.581
Pure Error	2	0.000459	0.000229	-	-	-
Total	16	0.010070	-	-	-	-
R-sq(adj) =**62.67**%	R-sq = 76.67**%**					

TABLE 6

Revised analysis of variance of exit hole circularity

Source	**DF**	**Adj SS**	**Adj MS**	**T-Value**	**F-Value**	**P-Value**
Model	5	0.041657	0.008331	-	6.49	0.005
Linear	٣	0.011986	0.003995	-	3.11	0.071
P	1	0.000729	0.000729	0.75	0.57	0.467
F	1	0.001056	0.001056	0.91	0.82	0.384
D	1	0.010201	0.010201	2.82	7.95	0.017
2-Way Interaction	2	0.029670	0.014835	-	11.56	0.002
P×D	1	0.010658	0.010658	-2.88	8.30	0.015
F×D	1	0.019012	0.019012	-3.85	14.81	0.003
Error	11	0.014123	0.001284	-	-	-
Lack-of-Fit	9	0.009427	0.001047	-	0.45	0.838
Pure Error	2	0.004695	0.002348	-	-	-
Total	16	0.055779	-	-	-	-
R-sq(adj) =**63.17**%	R-sq = 74.68**%**					

TABLE 7

Revised analysis of variance of hole taper

Source	**DF**	**Adj SS**	**Adj MS**	**T-Value**	**F-Value**	**P-Value**
Model	4	0.077866	0.019466	-	35.74	0.000
Linear	2	0.044460	0.022230	-	40.81	0.000
P	1	0.005301	0.005301	3.12	9.73	0.009
F	1	0.039158	0.039158	-8.48	71.90	0.000
Square	2	0.033406	0.016703	-	30.67	0.000
P×P	1	0.006359	0.006359	3.42	11.68	0.005
F×F	1	0.032510	0.032510	7.73	59.69	0.000
Error	12	0.006536	0.000545	-	-	-
Lack-of-Fit	10	0.005755	0.000575	-	1.47	0.471
Pure Error	2	0.000781	0.000391	-	-	-
Total	16	0.084402	-	-	-	-
R-sq(adj) =**89.68**%	R-sq = 92.26**%**					

TABLE 8

Constraints and criteria of input parameters and responses

No	Parameter/Response		Goal	Lower	Target	Upper	Weight	Importance
1	**Parameters**	Frequency	Is in range	80	---	240	---	---
2		duty cycle	Is in range	20%	---	40%	---	---
3		laser power	Is in range	100	---	200	---	---
4	**Responses**	D (ent)	Minimum	370.21	370.21	550.57	1	5
5		circularity of entrance hole	Maximum	0.749	0.841	0.841	1	5
6		Hole taper	Minimum	0.04	0.04	0.33	1	5
7		circularity of exit hole	Maximum	0.529	0.746	0.746	1	3

TABLE 9

Optimum prediction results and experimental validation

No	Optimum input parameters			Composite Desirability		Output responses			
	F (Hz)	D (%)	P (W)			D (ent) (µm)	circularity of entrance hole	hole taper (^{0})	circularity of exit hole
1	240	26.263	174.75	0.768706	Actual	398.83	0.7642	0.16802	0.6551
					Predicted	426.84	0.8328	0.1481	0.7464
					Error %	6.56	8.24	13.45	12.23